Development 135, 3301-3310 (2008) doi:10.1242/dev.022442

Teashirt 3 is necessary for ureteral smooth muscle differentiation downstream of SHH and BMP4

Xavier Caubit[1,*], Claire M. Lye[2,*], Elise Martin[1,*], Nathalie Coré[1], David A. Long[2], Christine Vola[1], Dagan Jenkins[3], Alistair N. Garratt[4], Helen Skaer[5], Adrian S. Woolf[2,†] and Laurent Fasano[1,†]

Ureteric contractions propel foetal urine from the kidney to the urinary bladder. Here, we show that mouse ureteric smooth muscle cell (SMC) precursors express the transcription factor teashirt 3 (TSHZ3), and that *Tshz3*-null mutant mice have congenital hydronephrosis without anatomical obstruction. Ex vivo, the spontaneous contractions that occurred in proximal segments of wild-type embryonic ureter explants were absent in *Tshz3* mutant ureters. In vivo, prior to the onset of hydronephrosis, mutant proximal ureters failed to express contractile SMC markers, whereas these molecules were detected in controls. Mutant embryonic ureters expressed *Shh* and *Bmp4* transcripts as normal, with appropriate expression of *Ptch1* and pSMAD1/5/8 in target SM precursors, whereas myocardin, a key regulator for SMC differentiation, was not expressed in *Tshz3*-null ureters. In wild-type embryonic renal tract explants, exogenous BMP4 upregulated *Tshz3* and myocardin expression. More interestingly, in *Tshz3* mutant renal tract explants, exogenous BMP4 did not improve the *Tshz3* phenotype. Thus, *Tshz3* is required for proximal ureteric SMC differentiation downstream of SHH and BMP4. Furthermore, the *Tshz3* mutant mouse model of 'functional' urinary obstruction resembles congenital pelvi-ureteric junction obstruction, a common human malformation, suggesting that *TSHZ*, or related, gene variants may contribute to this disorder.

KEY WORDS: Gene targeting, Teashirt 3 (Tshz3), UPJO, Ureter, Smooth muscle

INTRODUCTION

Diverse viscera contain contractile smooth muscle cells (SMC) and SM pathology is associated with several diseases, including asthma, lung fibrosis and liver cirrhosis. Thus, studies that unravel the molecular mechanisms regulating visceral SMC differentiation are potentially of great importance for understanding human disease. In the urinary tract, SM is present in the renal pelvis, the ureter, the bladder and the urethra, and is central to the functions of these organs. As in other viscera, ureteric SM develops from local mesenchyme (Yu et al., 2002) and hence the mouse ureter represents an appropriate paradigm to elucidate mechanisms controlling visceral SMC differentiation.

A dilated renal pelvis, or hydronephrosis, occurs in 0.9-7.7% of human gestations, the exact incidence depending on the criteria used to define the upper normal limit of the pelvic diameter (Ek et al., 2007; Gunn et al., 1995; Ismaili et al., 2006). Although most such dilatations are transient normal variants, others persist after birth and thus represent congenital malformations. In this context, a common diagnosis is unilateral or, less often, bilateral pelvi-ureteric junction obstruction (PUJO), present in up to 0.3-0.4% of all babies (Ek et al., 2007; Gunn et al., 1995; Ismaili et al., 2006). PUJO ureters are not anatomically blocked but have aberrant SM arrangement where the proximal ureter joins the renal pelvis (dell'Agnola et al., 1990; Zhang et al., 2000). Ureteric peristalsis propels urine from the renal pelvis towards the urinary bladder, and a failure of this activity causes 'functional' flow impairment leading to urinary tract dilatation and kidney damage (Mendelsohn, 2004). Peristalsis is propagated distally along the urinary tract by SM in the ureter coat. Therefore, failure in SM differentiation along the urinary outflow tract may be an important primary cause of functional obstruction and hydronephrosis.

Between mouse embryonic day (E) 10 and 11, the metanephric mesenchyme (MM) signals to the ureteric bud (UB) to promote its outgrowth from the mesonephric duct and entry into the MM. Thereafter, UB branching morphogenesis generates kidney collecting ducts, and UB branch tip signals induce MM cells to aggregate and undergo mesenchymal-to-epithelial transition, forming nephrons. Meanwhile the unbranched stalk of the UB outside the MM elongates to form the ureter tube epithelium, the 'urothelium', while surrounding mesenchymal cells also contribute to the ureter becoming the cells of the lamina propria, SM and connective tissue.

Reciprocal signalling between the epithelial and mesenchymal components of ureter is essential for correct ureter development (Airik and Kispert, 2007; Mendelsohn, 2006). UB stalk epithelia secrete sonic hedgehog (SHH), which has a proliferative effect on ureteric mesenchyme and induces bone morphogenetic protein 4 (BMP4) in peri-urothelial mesenchymal cells (Yu et al., 2002). Inactivation of *Shh* in the urinary tract delays ureteric SMC maturation and causes loss of stromal cells located between the urothelial and SM layers (Yu et al., 2002). BMP4 promotes the differentiation of ureteric mesenchyme into SMCs and also facilitates urothelial maturation (Brenner-Anantharam et al., 2007; Miyazaki et al., 2003; Raatikainen-Ahokas et al., 2000). In response to signals from ureteric mesenchyme, UB stalk epithelia mature into urothelia, and express uroplakin (UPK)-rich plaques on their apical surfaces to maintain the 'water-tight' properties of this epithelium (Jenkins and Woolf, 2007).

[1]Institut de Biologie du Développement de Marseille-Luminy (IBDML), UMR6216, CNRS, Université de la Méditerranée, F-13288 Marseille cedex 09, France. [2]Nephro-Urology Unit, UCL Institute of Child Health, 30 Guilford Street, London WC1N 1EH, UK. [3]Weatherall Institute of Molecular Medicine, University of Oxford, John Radcliffe Hospital, Oxford OX3 9DS, UK. [4]Max-Delbrueck-Center for Molecular Medicine, Robert-Roessle-Strasse 10, 13125 Berlin, Germany. [5]Department of Zoology, University of Cambridge, Downing Street, Cambridge CB2 3EJ, UK.

*These authors contributed equally to this work
†Authors for correspondence (e-mails: a.woolf@ich.ucl.ac.uk; fasano@ibdml.univ-mrs.fr)

Accepted 30 July 2008

Recently, other mouse models confirmed that, unless mesenchymal cells surrounding the ureter stalk differentiate normally, congenital malformations of the urinary tract will arise. The transcription factor TBX18 is expressed in undifferentiated mesenchymal cells around ureter. In *Tbx18*$^{-/-}$ mice, absence of condensation and differentiation of ureteral mesenchymal cells into SM results on congenital hydronephrosis (Airik et al., 2006). Deletion of a regulatory subunit of calcineurin, *Cnb1* (*Ppp3r1* – Mouse Genome Informatics) in the mesenchyme of the developing urinary tract results in reduced proliferation in the SMCs, leading to defective postnatal pyeloureteral peristalsis and renal obstruction (Chang et al., 2004). Despite these insights, there is still a crucial need to develop new mouse models for congenital ureter malformations to help understand the mechanisms that underlie SM differentiation.

In *Drosophila*, renal (Malpighian) tubules (MpTs) are major excretory and osmoregulatory organs. They derive from two cell populations, ectodermal epithelial buds and surrounding mesenchymal mesoderm, and unexpected parallels exist between MpTs development and vertebrate nephrogenesis (Denholm et al., 2003). Several fly MpT genes such as *Kr*, *cut*, *hibris* and *Odd* have vertebrate homologues (*Glis2*, *Cux1*, nephrin and *Osr*, respectively) implicated in kidney development (Sharma et al., 2004; Tena et al., 2007; Vanden Heuvel et al., 1996; Zhang et al., 2002). We have previously shown that stellate cells within MpT express two related zinc-finger transcription factors, *teashirt* (*tsh*) and *tiptop* (*tio*) (Denholm et al., 2003; Laugier et al., 2005). Furthermore, we found that the three mouse teashirt (Tshz) genes were functionally equivalent to *Drosophila tsh* in terms of rescuing homeotic and segment polarity phenotypes of a *tsh*-null mutant fly (Caubit et al., 2005; Manfroid et al., 2004).

Based on the above observations about the Tsh/Tshz families, we suspected that they might be expressed in, and have roles in, mammalian renal tract development. Here, we show that mouse ureteric SMC precursors express *Tshz3* and that *Tshz3*-null mutant mice have congenital hydronephrosis without anatomical obstruction. Ex vivo, the spontaneous contractions that occurred in proximal segments of wild-type embryonic ureter explants were absent in *Tshz3* mutant ureters. In vivo, prior to the onset of hydronephrosis, mutant proximal ureters failed to express contractile SMC markers, whereas these molecules were detected in controls. Mutant embryonic ureters expressed *Shh* and *Bmp4* transcripts, as normal, with appropriate expression of *Ptch1* and pSMAD1/5/8 in target SM precursors, whereas myocardin, a key regulator for SMC differentiation (Wang and Olson, 2004), was not expressed in *Tshz3* null ureters. In wild-type embryonic renal tract explants, exogenous BMP4 upregulated *Tshz3* and myocardin expression. Thus, *Tshz3* is required for proximal ureteric SMC differentiation downstream of SHH and BMP4.

MATERIALS AND METHODS

Gene targeting of the *Tshz3* locus

Tshz3 genomic DNA fragments were isolated from a 129/Ola mouse genomic library. To generate the targeting construct, we used a vector (pKO) containing a *neo*-resistance gene derived from the pMC1NeoPolyA vector (Mansour et al., 1988) flanked in 5′ with a multiple cloning site and separated in 3′ from the HSV-*tk* cassette by *Sal*I and *Bam*H1 sites. A 0.53 kb short arm, comprising the start of exon 2, was PCR generated and fused in frame with a *lacZ*-SV40polyA cassette excised from pETL as a 4.25 kb *Bam*HI fragment (Mombaerts et al., 1996). The 0.53 kb *lacZ* cassette was inserted 5′ to the *neo* gene and a 5.8 kb fragment 3′ of the *Tshz3* gene was inserted between the *neo* and HSV-*tk* genes of pKO. E14 (129/Ola) ES cells were electroporated with 20 μg of targeting vector and cultured in presence of 300 μg/ml G418 for positive selection. Two days later, negative selection was applied using 2 μM gancyclovir. The neomycin sequence was used as a probe to check unique integration event. Correct recombination 5′ to the locus was controlled by PCR using a forward primer upstream to the 5′ homology region, (5′TTACAAATAAATGCGCCCGT3′) and a reverse primer in the *lacZ* gene (5′CCTCTTCGCTATTACGCCAG3′).

Generation of *Tshz3*-null mice

Animals were treated according to protocols approved by the French Ethical Committee. Male chimeras, generated after injection of *Tshz3*$^{lacZ/+}$ ES cells into C57BL/6J blastocysts, were mated to C57BL/6J females. Offspring (*n*=249) were assayed for germline transmission of the *Tshz3*^{lacZ} allele but no transmission was PCR detected. Male chimeras were then mated to CD1 females. F1 *Tshz3*$^{lacZ/+}$ animals were intercrossed to obtain *Tshz3*$^{lacZ/lacZ}$ mutant mice. Alternatively, F1 *Tshz3*$^{lacZ/+}$ males were crossed to CD1 females to generate *Tshz3*$^{lacZ/+}$, and mutant mice were analysed after six generations on the CD1 background. Genomic DNA was PCR-genotyped. Primers (5′GGAAGGGACTGGCTGCTATTG3′ and 5′CGATACCGTAAAGCACGAGG3′) for the *neo* sequence amplified a 478 bp fragment from the recombinant allele, and primers for exon 2 (5′CGGAGCATCTGGACCGCTATT3′ and 5′CTGATATACGTGGAAGGAGTC3′) amplified a 630 bp fragment from the wild-type allele. Representative and reproducible morphology and gene/protein expression patterns based on four to 20 embryos for each genotype at each embryonic stage are shown.

Immunoprobing and in situ hybridisation

Tissues were fixed in 4% paraformaldehyde. Paraffin-embedded sections (5-10 μm) were stained with Haematoxylin and Eosin or Masson's trichrome. X-Gal staining was performed as described (Relaix et al., 2004). Immunostaining was performed either on 14 μm cryosections of tissues or on paraffin-embedded sections after quenching endogenous peroxidase and antigen retrieval followed by reaction with secondary antibodies (details available on request). Whole explants were blocked in 5% goat serum/PBS/0.3% Triton X-100 then incubated with mouse anti-smooth muscle α actin (SMAA; Sigma, clone 1A4; 1/1000) and rabbit anti-E-cadherin (G. Rougon, IBDML-France; 1/500) antibodies. Guinea-pig anti-TSHZ3 antibody (1/5000) was raised against mouse amino acids 557-664, cloned as a His-tagged fusion protein in pET14b (Novagen) and produced by A. Garratt's laboratory. Other primary antibodies were: rabbit anti-β-galactosidase (Cappel; 1/1000); rabbit anti-Pax2 (Zymed; 1/50); mouse anti-proliferating cell nuclear antigen (PCNA; BD Pharmingen; 1/200); rabbit anti-pSMAD1/5/8 (Cell Signaling; 1/200); rabbit anti-retinaldehyde dehydrogenase 2 (RALDH2; 1/2000) (P. McCaffery, University of Aberdeen, UK); goat anti-myocardin (sc-21559; Santa-Cruz; 1/200); rabbit anti-aquaporin 2 (Chemicon; 1/400); sheep anti-uromodulin (Biodesign, AMS Biotechnology Distribution; 1/500); rabbit anti-SM myosin heavy chain (SMMHC; anti-MHC204/200; 1/500; M. Conti and R. Adelstein, Laboratory of Molecular Cardiology, Bethesda, USA) (Kelley et al., 1991); rabbit anti-SM protein alpha 22kDA (SM22a; 1/1000) (M. Gimona, Austrian Academy of Sciences, Salzburg, Austria); and rabbit antiserum to total UPK (1/100; T. T. Sun, New York School of Medicine, USA). Apoptotic cells were detected using the In Situ Death Detection Kit (Roche). For each sample, the number of apoptotic cells, and the total number of cells were counted for each of the following cell populations in the proximal ureter: urothelium, aggregated mesenchyme and loose mesenchyme.

India ink solution was injected into renal pelves as described previously (Airik et al., 2006). In situ hybridisation using digoxigenin-labelled or radioactive probes was performed on sections as described (Caubit et al., 2005). Probes used were: *Bmp4* (B. Hogan, Duke University, Durham, USA); *Ptch1* (M. Scott, HHMI, Stanford University School of Medicine, USA); *Shh* (D. Epstein, University of Pennsylvania School of Medicine, USA); *Smaa* and *Myocd* (E. Oslon, University of Texas Southwestern Medical Center, Dallas, USA); *foxd1* (A. Kispert, Medizinische Hochschule Hannover, Germany); and *Raldh2* (J. Xavier-Neto, HC.FMUSP, São Paulo-SP, Brazil).

Embryonic ureter culture and video microscopy

E15.5 ureters were dissected and explanted onto platforms (Millipore; pore size 0.4 μm) and cultured in defined, serum-free media, as described for embryonic mouse urinary bladders (Burgu et al., 2006). The timelapse imaging is detailed in the movie legends (see supplementary material). Images were analysed using Metamorph software.

Metanephric explant cultures

Kidney rudiments were isolated and cultured as described (Brenner-Anantharam et al., 2007). Explants, each consisting of a metanephros and an attached ureter, were isolated from E12.5 mouse embryos and cultured for 96 hours. For real-time quantitative PCR (qPCR) analyses, explants were isolated from E13.5 mouse embryos and cultured for 72 hours. In some cultures, 100 ng/ml recombinant BMP4 (R&D Systems) was added to the culture medium. In all cases, medium was changed daily. RNA was isolated using TRIsure Reagent (Bioline) according to the manufacturer's instructions. Total RNA was reverse-transcribed using iScript cDNA synthesis kit (Bio-Rad Laboratories). Real-time PCR was performed on a PTC-200 DNA Engine Opticon System (Bio-Rad Laboratories) using iQ SYBR Green Supermix (Bio-Rad Laboratories). Primer sequences used for Sybr RT-PCR are as follows: *Tshz3*, 5′-gcgcgcagcagcctatgtttc and 3′-tcagccatccggtcactcgtc; *Myocd*, 5′-caaggcttaataccgccactg and 3′-aatgtgc-atagtaaccaggctg; *Id3*, 5′-agcttagccaggtggaaatcct and 3′-tcagctgtctggatc-gggag. Results were normalised to *Hprt* expression.

RESULTS

Tshz3 is expressed in mesenchymal populations of the developing urinary tract

Using an anti-TSHZ3 antibody, we looked at the spatial distribution of the TSHZ3 protein in developing metanephros (Fig. 1). The expression patterns were confirmed by in situ hybridisation analyses (not shown). At E11.5 TSHZ3-expressing cells were noted around the UB stalk (Fig. 1A). At E12.5, TSHZ3 was expressed in mesenchymal cells along and around the UB stalk, and was absent from the UB epithelium that itself expressed PAX2 (Schedl, 2007) (Fig. 1B). At E12.75, in addition to the expression in the nascent ureteric mesenchyme, TSHZ3 was detected in scattered cells within the metanephric medullary stroma (Fig. 1C). At E15.5, TSHZ3 expression was noted in mesenchymal cells of the ureter and renal pelvis, and in renal medullary stroma; the outer rim of nephrogenic mesenchyme was negative (Fig. 1D). At this stage, transverse sections of the ureter revealed that TSHZ3 was detected in mesenchymal cells condensed around urothelia, and also in loosely organised cells with cell bodies arranged tangentially (Fig. 1E). In the E15.5 bladder, TSHZ3 was detected in rare mesenchymal cells adjacent to the epithelium and in the peripheral mesenchyme where SM starts to differentiate (Fig. 1F) (Li et al., 2006). At E18.5, TSHZ3 expression was maintained in ureteric mesenchymal cells, including those directly subjacent to the ureteral epithelium, where stromal cells are located (Fig. 1G). In the E18.5 bladder, TSHZ3 was found in the (submucosal) loose connective tissue adjacent to the epithelium and in the detrusor SM layer (Fig. 1H). These expression patterns are consistent with the hypothesis that the TSHZ3 transcription factor plays roles in renal tract development.

Generation of mice containing a null mutation of *Tshz3*

To address the issue of the functional contribution of *Tshz3* in the developing renal tract, we generated mice homozygous for a null mutation in the *Tshz3* gene ($Tshz3^{lacZ}$) (Fig. 2A-D). Chimeras were mated to CD1 females and seven chimeras achieved germline transmission. Crossing $Tshz3^{lacZ/+}$ parents failed to produce viable null mutant offspring but genotyping E18.5 litters showed that homozygous mutants ($Tshz3^{lacZ/lacZ}$) developed at the expected Mendelian ratio. E18.5 $Tshz3^{lacZ/lacZ}$ embryos obtained after Caesarian section became cyanotic and died within 1 hour. They showed no external anatomical differences from the wild types, but they did not move spontaneously and reacted only to strong stimuli. $Tshz3^{lacZ/lacZ}$ lungs sunk, whereas control lungs floated on water (data not shown). Thus, $Tshz3^{lacZ/lacZ}$ animals die because of an inability to breathe. The rapid death is unlikely to be associated with renal tract defects described below because even severe kidney excretory failure is not fatal for at least 1 day. Instead, it is likely that *Tshz3* is also necessary for respiration and this is the focus of a separate investigation.

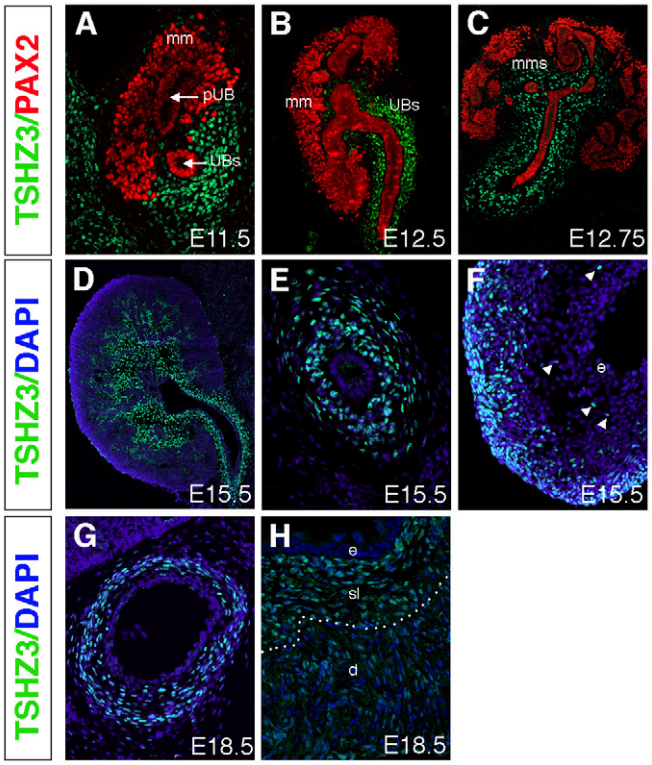

Fig. 1. Expression of TSHZ3 in the developing ureter and metanephros. (**A-C**) Immunostaining for TSHZ3 (green) and PAX2 (red) that visualises the UB and metanephric mesenchyme (mm) at E11.5 (A), E12.5 (B) and E12.75 (C). (**D-H**) Immunostaining for TSHZ3 (green) and nuclei (DAPI, blue) at E15.5 in metanephros (D), ureter (E) and bladder (F) and at E18.5 in ureter (G) and the bladder (H). Broken line in H separates the submucosal layer and the detrusor. d, detrusor SM; e, epithelium; mm, metanephric mesenchyme; mms, metanephric medullary stroma; pUB, proximal ureteric bud; sl, submucosal layer; UBs, ureteric bud stalk.

Using comparative analysis on whole mounts and tissues sections, we confirmed that the expression of the $Tshz3^{lacZ}$ allele recapitulated the expression pattern of endogenous *Tshz3*, providing evidence that the *Tshz3* gene was correctly targeted. Part of this analysis is illustrated in Fig. 2, where TSHZ3 and β-galactosidase (β-gal) were detected in periureteral mesenchymal cells and excluded from the epithelium in transverse sections of E14.5 ureters; inactivation of the *Tshz3* locus was attested by the absence of TSHZ3 protein in $Tshz3^{lacZ/lacZ}$ (Fig. 2E).

Inactivation of *Tshz3* causes hydroureter and SMCs malformation

Mutant urinary tracts displayed a prominent proximal hydroureter and the kidneys were markedly hydronephrotic (Fig. 3B,C): a fully penetrant bilateral phenotype evident from E16.5 that affects both sexes. In heterozygous embryos, rare cases (4/80) of unilateral hydroureter occurred. Histological analysis confirmed dilation of the renal pelvis in null mutants (Fig. 3D,E) and showed that the dilated proximal ureters were thin-walled (Fig. 3I,J). In wild-type ureters,

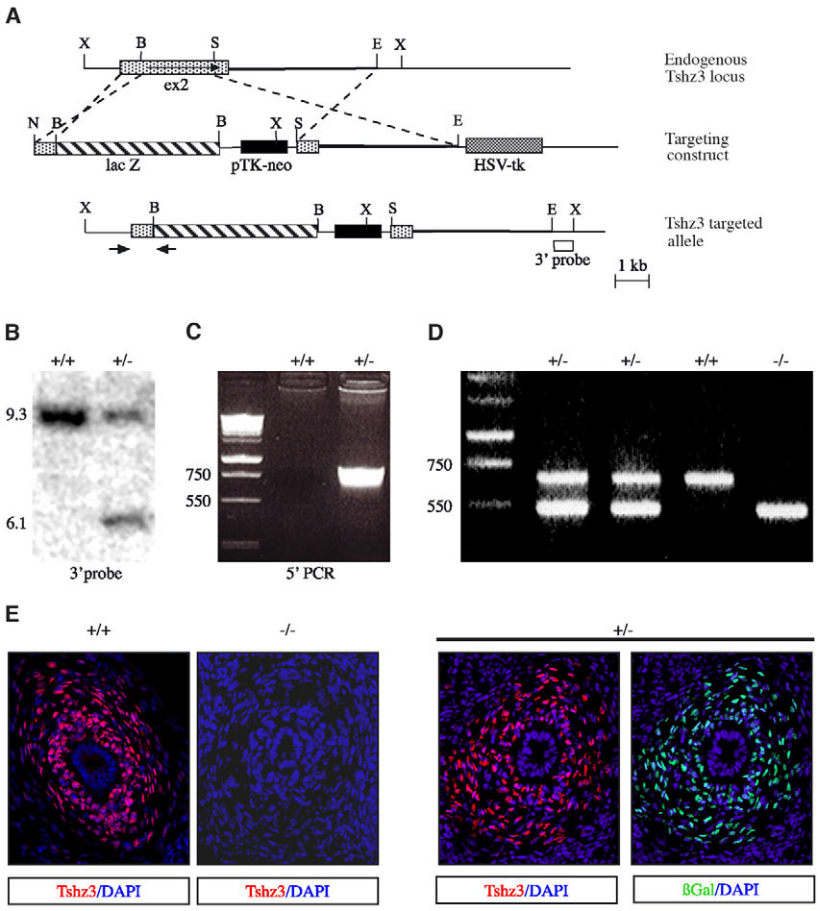

Fig. 2. Targeted disruption of *Tshz3*. (**A**) Gene targeting strategy. The mouse *Tshz3* locus consists of two exons and one intron, and spans more than 75 kb; the first and second exons encode, respectively, 13 and 1068 amino acids. The in-frame insertion of the *lacZ*-coding sequence (hatched box) and the *neomycin* expression cassette (*pTK-neo*; black box) into exon 2 (ex2; light dotted box) resulted in complete deletion of the zinc-finger motifs and created an *Xba*I digest size difference between wild-type and targeted loci. Restriction sites are abbreviated as follows: B, *Bam*HI; E, *Eco*RI; S, *Sal*I, N, *Not*I, X, *Xba*I. (**B**) Southern blot analysis of DNA from wild-type (+/+) and targeted (+/–) ES cell clones using *Xba*I-digested genomic DNA and a 3′ external probe (3′ probe; white box in A). (**C**) Appropriate recombination 5′ to the locus was confirmed by PCR with primers shown in A (short arrows). (**D**) PCR-based genotyping of wild-type (+/+), heterozygous (+/–) and homozygous null (–/–) embryos. (**E**) Immunostaining of TSHZ3 (left panel) on sections from E15.5 wild-type (+/+) and $Tshz3^{lacZ/lacZ}$ mutant (–/–) ureter; TSHZ3 is not detected in mutant ureter. Co-immunostaining of TSHZ3 and β-gal (right panel) on a section from E14.5 $Tshz3^{lacZ/+}$ heterozygote ureter.

the multilayered epithelium was surrounded by condensed mesenchymal cells that differentiated into multiple SM layers (Fig. 3F,G). Close inspection of $Tshz3^{lacZ/lacZ}$ proximal ureters revealed that the structural organisation of these muscular layers was lost, leading to a thin layer of mesenchymal cells. The urothelium was present but arranged in a monolayer as a consequence of the distension of the proximal ureter (Fig. 3I,J). However, the distal ureter did not appear to be affected because mesenchymal cell layers were properly organised and the urothelium multilayered as normal (Fig. 3H,K).

Other than being hydronephrotic, E18.5 null mutant kidneys were similar to wild type (see Fig. S1 in the supplementary material). We then assessed the expression patterns of several genes expressed in subsets of cells in the mammalian kidney. We observed condensing nephrogenic MM in the outer cortex and several layers of podoplanin-expressing glomeruli (Breiteneder-Geleff et al., 1997) in the deeper cortex; transcripts of cortical stromal genes *Foxd1* and *Raldh2* (Schmidt-Ott et al., 2006) were normally expressed, as was the Pax2 transcription factor, which was detected in nuclei of MM condensations and in UB branch tips (Winyard et al., 1996). Within the medulla of the E18.5 kidney, similar expression patterns in wild types and mutants were detected for SMAA, which is normally transiently expressed in interstitial cells (Chung and Chevalier, 1996), for the collecting duct markers Pax2 (Winyard et al., 1996) and aquaporin 2 (Marples et al., 1995), and for uromodulin, a marker of the thick limb of the ascending loop of Henle (Hoyer et al., 1974). The morphology and histology of the bladder were not affected in $Tshz3^{lacZ/lacZ}$ (see Fig. S2A,B in the supplementary material).

To determine the onset of urinary tract malformations in $Tshz3^{lacZ/lacZ}$, we harvested embryos from timed mating and analysed urinary tract histology. From E12.5, we observed that the mesenchymal progenitors condensed as normal around the ureteric epithelium until E15.5 (data not shown) (see Fig. S2G,H in the supplementary material). However, at E16, as hydroureter developed, peri-urothelial cells appeared less organised compared with wild-type ureters (Fig. 3L-O).

Analysis of E18.5 mutant urinary tracts by India ink injection revealed no sign of physical obstruction: ink flowed down the ureter into the bladder, suggesting that hydroureter and hydronephrosis were caused by functional, rather than by anatomical, obstruction (Fig. 3P-R). Furthermore, because the structural organisation of ureteric muscle is lost in $Tshz3^{lacZ/lacZ}$ embryos, our results suggest that *Tshz3* could play a role in ureteric SMC differentiation.

Lack of *Tshz3* perturbs peristalsis in forming ureters

To test for functional obstruction, which is caused by impaired peristalsis, we studied cultured embryonic ureters. When maintained in culture for up to 6 days, wild-type E15.5 ureters elongated and underwent spontaneous contractions several times/minute (Fig. 4A; see Movie 1 in the supplementary material). Contractions initiated approximately one-fifth of the way down the ureter and were followed by distal propagation: the most proximal parts of the explants also contracted immediately after the initiation of peristalsis (Fig. 4C) and, in vivo, this would probably ‘squeeze’ the renal papilla, which protrudes into the pelvis and proximal ureter. Null mutant ureters explanted at E15.5 (when urinary tract dilatation is not yet

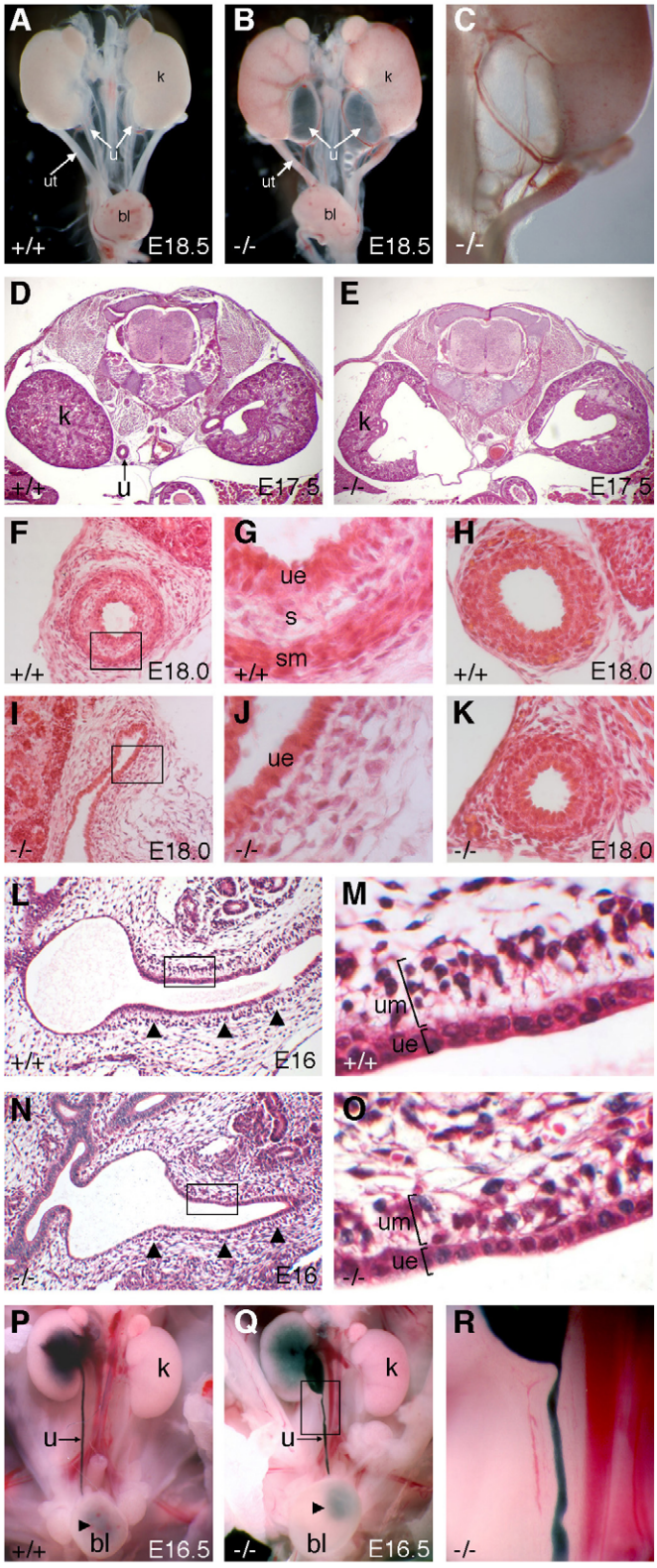

Fig. 3. *Tshz3*$^{lacZ/lacZ}$ mice develop congenital hydronephrosis. (**A**,**B**) Whole E18.5 urinary tracts. In comparison with wild-type littermates (A), *Tshz3*$^{lacZ/lacZ}$ kidneys had bilateral hydronephroses (B). (**C**) Higher magnification view of proximal hydroureter shown in B. (**D-K**) Haematoxylin and Eosin-stained transverse sections through E17.5 embryos (D,E) and E18.0 ureters (F-K). Wild-type proximal (F,G) and distal (H) ureter. *Tshz3*$^{lacZ/lacZ}$ proximal (I,J) and distal (K) ureter. The mutant ureter shown in I has collapsed post mortem, which is why it does not look dilated. (**L-O**) Sections are stained with Masson's trichrome and Haematoxylin which results in a red colour for muscles, blue for nuclei and a blue/green for collagens (epithelia also appear red). E16.0 wild-type (L) and mutant (N) ureters with mesenchymal cells surrounding proximal ureter ephithelia indicated by arrowheads. (M,O) High-power magnification images of longitudinal sections from wild-type (L) and *Tshz3*$^{lacZ/lacZ}$ (N) E16.0 proximal ureters demonstrate aggregating mesenchyme in wild type and early disorganisation of mesenchymal cells in mutants. (**P**,**Q**) E16.5 autopsies in which India ink was injected into the right renal pelvis of a normal (P) and a null mutant (Q) mouse: in both, ink flowed into the bladder (arrowhead). (**R**) Inset shows dilated proximal ureter filled with ink. bl, bladder; k, kidney; s, stromal layer; u, ureter; ue, ureteric epithelium; um, ureteral mesenchyme; ut, uterus.

present) also grew, initiated contractions at a similar proximal/distal level and propagated a pulse-wave distally. Significantly, however, null mutant proximal ureters completely failed to contract (Fig. 4D; see Movie 2 in the supplementary material). This result strongly supports the hypothesis that abnormal peristalsis of the proximal part of the ureter occurs in vivo, causing a functional obstruction that leads to hydronephrosis and hydroureter.

Tshz3 is expressed in differentiating SMCs

To better characterise the *Tshz3*-positive cell population, we performed double immunostaining for β-gal (to report the expression of *Tshz3*) and SMAA, a marker of SMCs. In wild types, strong expression of SMAA has been reported at E15.5 in the condensed mesenchymal cells of the proximal ureter (Yu et al., 2002). In E15.5 heterozygous proximal ureters, we observed SMAA/β-gal double-positive cells in the condensed mesenchymal layer adjacent to the epithelium (Fig. 5B). In addition, β-gal was detected in loose mesenchymal cells excluded from the SMAA-positive layer, indicating that *Tshz3* was expressed both in undifferentiated mesenchymal cells far from the urothelium and in differentiating SMCs. At E18.5, β-gal expression was sustained in SMCs and in fewer mesenchymal cells at the periphery (Fig. 5D). From E18.5 onwards, we also detected β-gal expression within cells directly adjacent to the urothelium that were not positive for SMAA (Fig. 5D,F). These cells are thought to be progenitors of ureteral connective tissue and express *Raldh2* (Mahoney et al., 2006). At E18.5, cells double-positive for RALDH2 and β-gal activity were detected adjacent to the epithelium, suggesting that *Tshz3* marks progenitors of ureteral connective tissue (Fig. 5G). Together, these data confirmed that *Tshz3* is expressed in the SM of the developing ureter, and in other ureteric mesenchymal cell populations.

Tshz3 deficiency causes perturbed development of ureteric SMC

To test whether the hydronephrosis and hydroureter observed in the *Tshz3* mutant were caused by abnormalities in the SM, we examined SMCs development in *Tshz3*$^{lacZ/lacZ}$ ureters. A hallmark of SMCs differentiation is the elevated expression of SMC-selective differentiation marker genes, including *Smaa*, *Smmhc* and *Sm22a* (Owens, 1995). The differentiation of SM in the mouse ureter and the pelvis has been documented to occur in a proximodistal wave (McHugh, 1995; Yu et al., 2002). In wild-type embryos, SMAA is first detected at E14.5 in few cells within aggregated mesenchyme of the proximal ureter and the nascent renal pelvis (data not shown)

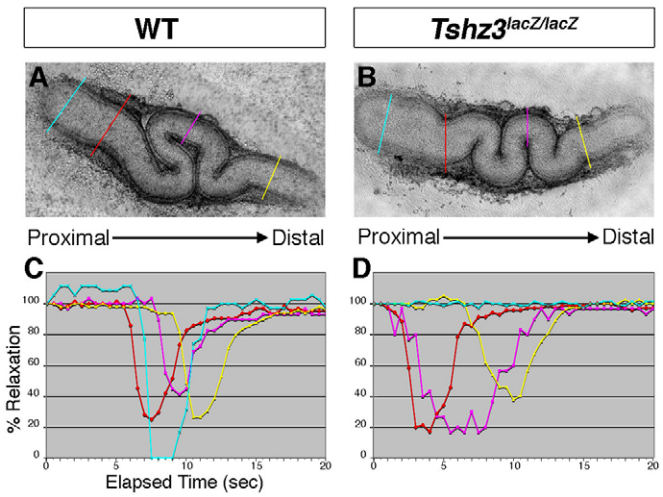

Fig. 4. Tshz3 is required for harmonised ureteric peristalisis. (**A**,**B**) Cultured ureter of wild-type (A) and *Tshz3*$^{lacZ/lacZ}$ (B) embryos. (**C**,**D**) Graphs illustrating peristaltic contractions of cultured ureters of wild-type (C) and *Tshz3*$^{lacZ/lacZ}$ (D) ureters. Measurements of luminal diameters were made at four different positions from their proximal to distal ends from a 20-second digital recording of contracting ureters (see Movies in the supplementary material). Data are presented as the percentage of the relaxed diameter. In the trace from the wild-type ureter (C), the contraction (downward motion from baseline) initiates about one-fifth of the way down (red line) the ureter; this is rapidly followed by both contraction of the more proximal segment (blue line) and also by distal propagation (pink and yellow lines). Null mutant trace (D) shows absent proximal segment contraction together with a variable delay of distal relaxation (pink line). Representative traces are shown for at least five samples from each genotype.

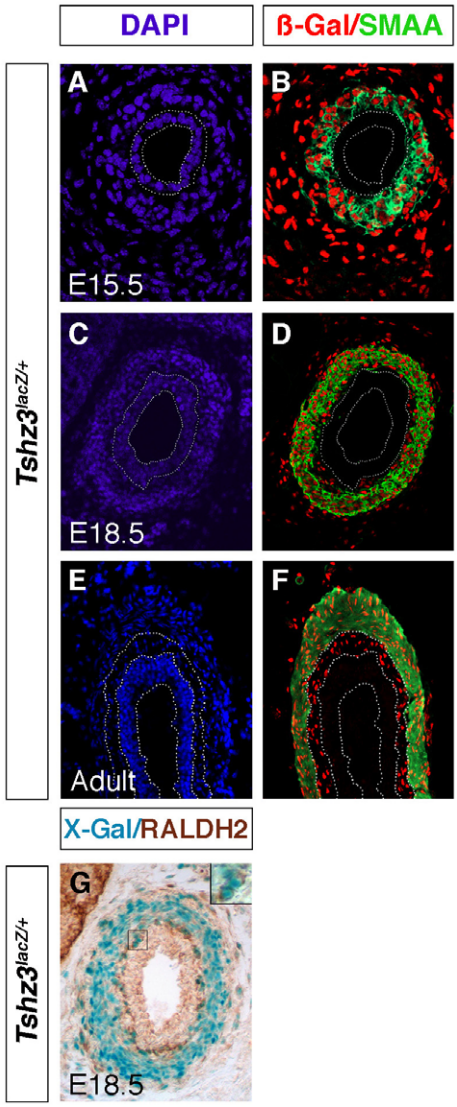

Fig. 5. Characterisation of Tshz3-positive mesenchymal cells in the developing ureter. (**A-F**) Immunostaining for SMAA (green) and β-gal (red) in tissue section of E15.5 (B), E18.5 (D) and adult (F) *Tshz3*$^{lacZ/+}$ ureters. Corresponding DAPI staining are shown (A,C,E). (**G**) Expression of *Tshz3* in E18.5 ureter from *Tshz*$^{lacZ/+}$ mice, revealed by X-Gal staining (blue) and immunohistochemistry for RALDH2 (brown): inset shows RALDH2/X-Gal double-positive cells.

(see also Yu et al., 2002). Examination of proximal ureters of E15.5 *Tshz3*$^{lacZ/lacZ}$ mutant embryos revealed almost absent expression of SMC contractile proteins, including SMAA, SMMHC and SM22 (Fig. 6D-F) versus controls embryos (Fig. 6A-C).

In vivo, in vascular SMC, the expression of genes encoding SMAA, SMMHC and SM22 depends on myocardin (Huang et al., 2008; Li et al., 2003). At E15.5, wild-type ureteric mesenchymal cells co-expressed MYOCD and SMAA proteins (Fig. 6G), and in situ hybridisation revealed *Myocd* expression in ureteral mesenchymal cells (Fig. 6H). By contrast, expression of *Myocd* was deficient in *Tshz3*$^{lacZ/lacZ}$ proximal ureters (Fig. 6K), correlating with absent expression of *Smaa* transcripts (Fig. 6I,L) and MYOCD and SMAA proteins (Fig. 6J). Crucially, at this timepoint, urinary tract dilatation was not yet present, so the observed downregulation of SMC marker expression in the mutant could not be a secondary effect resulting from hydroureter-related distortion. In wild types at E17.5, SMAA immunostaining revealed that proximal ureteric SMC layers became more organised and thicker (Fig. 6M). By contrast, in *Tshz3*$^{lacZ/lacZ}$ mutants, we observed that SMAA expression was lost in the proximal-most ureter (Fig. 6O) where the dilatation was prominent. Similar aberrant expression patterns were noted with SMMHC and SM22 (data not shown). However, in the distal-most part, where the diameter of the *Tshz3*$^{lacZ/lacZ}$ ureter was normal, SMAA was detected in the mesenchymal cells although at a lower level than in wild types (Fig. 6N,P), perhaps correlating with an apparently slower distal propagation of contraction wave ex vivo (note the longer contraction at the 'red' level in the mutant versus the wild-type ureter depicted in Fig. 4C,D). In *Tshz3*$^{lacZ/lacZ}$ bladders, SMA was normally expressed (see Fig. S2C-F in the supplementary material). Taken together, these data are consistent with the idea that TSHZ3 regulates expression of *Myocd* in visceral tissue, and that, as in vascular SMCs, expression of SM-specific genes in ureteric SMCs depends on *Myocd*.

Next, we determined whether the failure of SMC development might reflect defects in proliferation and/or apoptosis of periureteric cells (see Fig. S3 and Table S1 in the supplementary material). As assessed by PCNA immunostaining (see Fig. S3A,B in the supplementary material), we recorded no significant difference in proliferation between wild-type and mutant proximal ureters. As assessed by TUNEL analyses, apoptosis was never detected in aggregated cells around the urothelium in either genotype, whereas

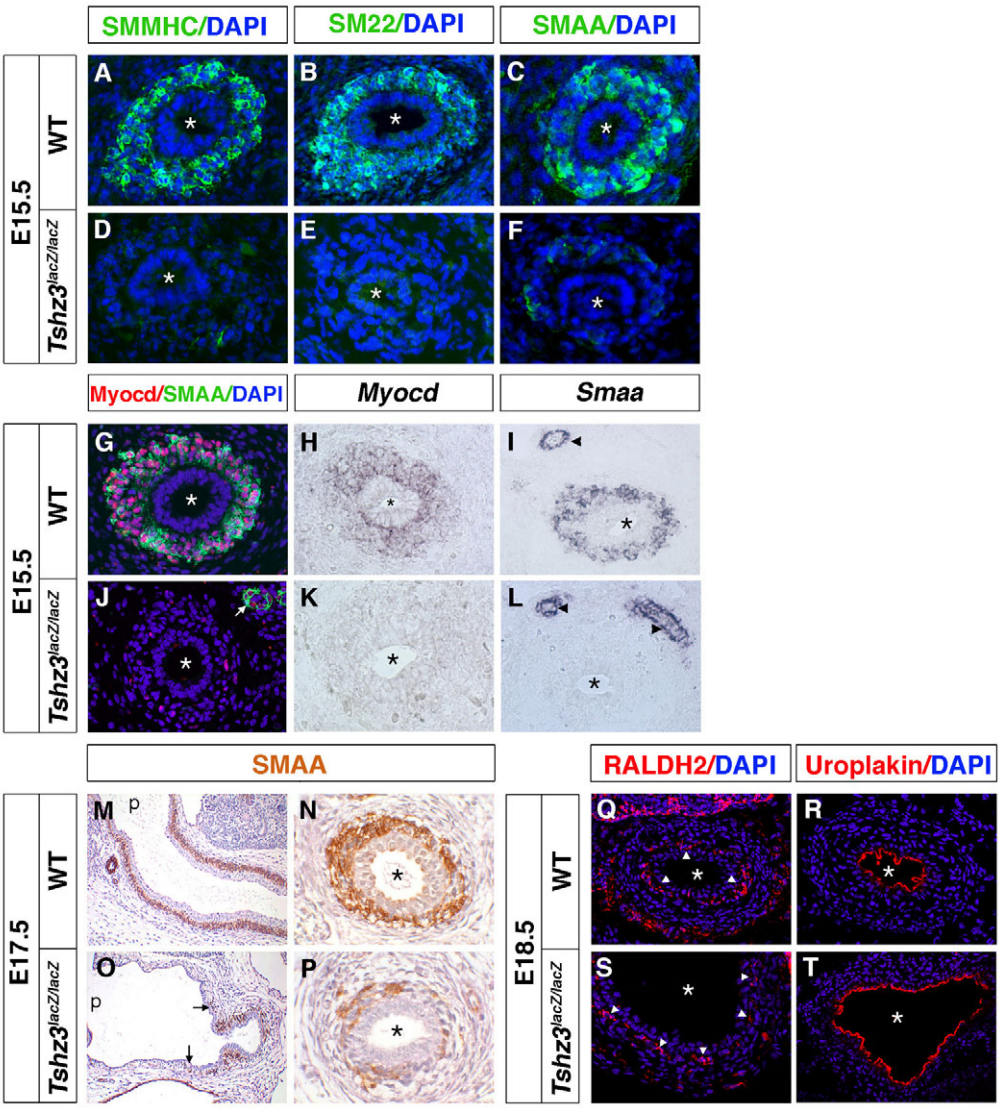

Fig. 6. Ureteric SMC differentiation in wild-type and *Tshz3*-null mutants. (**A-L**) Transverse sections of E15.5 proximal ureters. In A-F, all nuclei were stained with DAPI (blue) and immunohistochemistry (green positive signals) is shown for SMMHC (A,D), SM22 (B,E) and SMAA (C,F). (G,J) Sections from wild-type (G) or null mutant (J) immunostained for SMAA (green), MYOCD (red) and DAPI (blue); arrow in J indicates MYOCD- and SMAA-positive cells in artery. In situ hybridisation for *Myocd* (H,K) and *Smaa* (I,L) (positive purple signal): arrowheads in I and L indicate the *Smaa*-positive signal in arteries. (**M-P**) Longitudinal (M,O) and transverse (N,P) sections were counterstained with Haematoxylin (blue) and immunostained for SMAA (brown). In *Tshz3* mutant ureter (O) at E17.5, no SMAA was detected in the proximal ureter, in contrast to wild-type ureter (M). Distally, the immunostaining for SMAA was reduced in mutant (P) versus wild-type (N) ureters. (**Q-T**) E18.5 proximal ureter sections from wild-type (Q,R) or null mutant (S,T) stained with DAPI (blue) and immunostained for RALDH2 (Q,S, red) or UPK (R,T, red). Asterisks indicate the lumen of the ureter; arrowheads in Q and S indicate RALDH2-positive cells.

there was a similar, low prevalence in urothelia and also mesenchymal cells outside the aggregated mesenchymal layer. Furthermore, comparison of expression between *Tshz3*$^{lacZ/+}$ and *Tshz3*$^{lacZ/lacZ}$ ureters revealed similar numbers of β-gal-positive cells in both genotypes (see Fig. S3C,D in the supplementary material). Thus, *Tshz3* was not essential for SMC precursor proliferation or survival.

Because we found that *Tshz3* is expressed in RALDH2-positive cells, we investigated whether *Tshz3* was also involved in differentiation of these cells. At E18.5, RALDH2-positive cells were present in the dilated part of the *Tshz3* mutant ureter, but were scattered and did not form a continuous layer, probably as a consequence of the dilation caused by the hydroureter phenotype (Fig. 6Q,S). Distal to the dilated part, RALDH2-positive cells form a continuous layer as in wild-type ureter (not shown). In conclusion, loss of *Tshz3* does not affect the differentiation of the ureteric stromal cells, although their distribution is compromised.

Recent studies suggest that a signal from the ureteric mesenchyme to the ureteric epithelium participates in the differentiation of the urothelium (Airik et al., 2006). To investigate whether loss of *Tshz3* in the ureteric mesenchyme would compromise differentiation of the ureteric epithelium, we analysed UPK expression in E18.5 *Tshz3*$^{lacZ/lacZ}$ proximal ureters. Expression in both mutant and wild-type urothelium indicated that, despite failed SMCs differentiation, urothelia matured normally (Fig. 6R,T).

Tshz3 is downstream to SHH and BMP4 with regard to ureteric SMC differentiation

SHH signalling plays an essential role in ureteric SMC development by promoting proliferation of ureteric mesenchymal cells and inducing them to secrete BMP4; BMP4 in turn promotes SMC differentiation and *Bmp4*$^{+/-}$ mice exhibit hydroureter (Brenner-Anantharam et al., 2007; Miyazaki et al., 2000; Yu et al., 2002). We sought evidence for SHH signalling by in situ hybridisation for *Shh*, *Ptch1* and *Bmp4* in *Tshz3*$^{lacZ/lacZ}$ proximal ureters. *Shh* was expressed by E15.5 urothelia of both wild type and *Tshz3*$^{lacZ/lacZ}$, and *Ptch1* and *Bmp4* were expressed in peri-urothelial cells in both genotypes (Fig. 7A-F). In addition, we analysed the phosphorylation of SMAD proteins considered as mediators of BMP signal transduction (Massague et al., 2005). At E14.5, similar levels of nuclear pSMAD1/5/8 protein were detected in periureteral mesenchymal cells in wild-type and *Tshz3* mutant proximal ureters (Fig. 7G,H). Taken

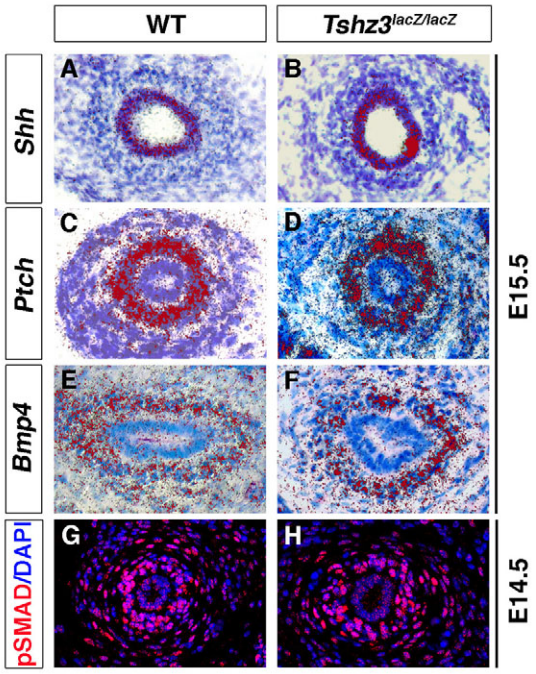

Fig. 7. Molecular characterisation of *Tshz3*$^{lacZ/lacZ}$ ureters. (**A-F**) In situ hybridisation on transverse sections of E15.5 proximal ureters of wild type (A,C,E) and *Tshz3*-null mutant (B,D,F). Patterns of expression (red dots) were similar in both genotypes, with *Shh* expressed in urothelia (A,B), and *Ptch1* (C,D) and *Bmp4* (E,F) expressed in peri-urothelial cells. Silver grains were pseudo-coloured in Adobe Photoshop. (**G**,**H**) E14.5 proximal ureter sections from wild type (G) or null mutant (H) immunostained for pSMAD 1/5/8 (red) and DAPI (blue).

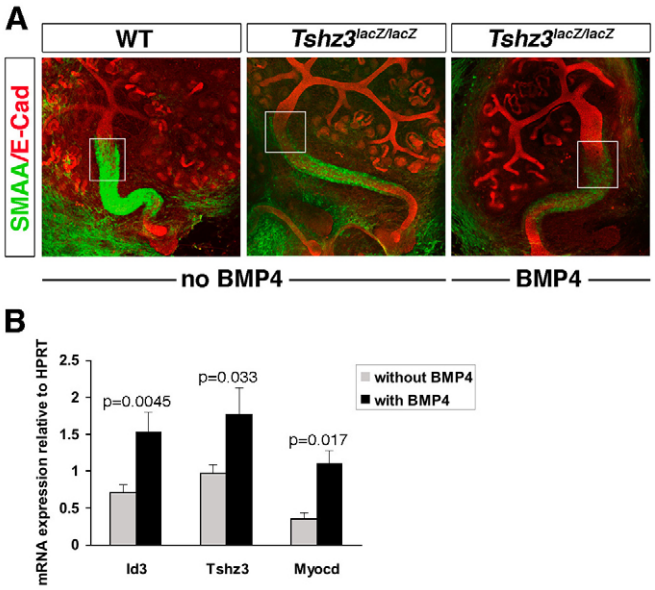

Fig. 8. *Tshz3* induction by BMP4. (**A**) Whole-mount images of E12.5 explants (each comprising a metanephros and attached ureter) cultured for 4 days in absence (left and middle panels) or in presence (right panel) of recombinant BMP4 (100 ng/ml). Ureters were immunoprobed with antibodies directed against SMAA (green) and E-cadherin (red; E-Cad) to detect SMC and epithelia, respectively. In each frame, the proximal ureter is outlined by a box; note the paucity of SMAA expression in this region in the mutants, whether or not exposed to exogenous BMP4. (**B**) Effects of BMP4 on gene expression in E13.5 wild-type explants cultured for 3 days in absence or presence of exogenous BMP4 (100 ng/ml). After factoring for *Hprt*, real-time Q-PCR revealed significant increases for *Id3, Tshz3* and *Myocd*. Statistical analyses were performed by one-tailed paired *t*-tests. Expression data are represented as mean±s.e.m. with n=5 in each group.

together, these results indicate that *Tshz3* mutant mesenchyme was directly responding to SHH and BMP4 signalling, in the same way as wild-type cells, even though they failed to form SMC.

To investigate whether addition of BMP4 could restore SMAA in absence of TSHZ3, we cultured renal tract rudiments with, or without, exogenous BMP4 protein (Fig. 8A). In wild types without added BMP4, both the proximal and distal ureter robustly expressed SMAA. *Tshz3*$^{lacZ/lacZ}$ explants cultured without exogenous BMP4 displayed little SMAA immunoreactivity in the proximal ureter, although some was expressed distally; furthermore, exogenous BMP4 did not 'rescue' SMAA expression (Fig. 8A). In other experiments, we tested whether exogenous BMP4 might alter the levels of transcripts for *Tshz3*, *Myocd* and also *Id3*, a gene known to be upregulated by BMP4 (Shepherd et al., 2008) and expressed in embryonic renal tracts (Jen et al., 1996). As assessed by qPCR, expression of all three genes was significantly upregulated after exposure of explants to BMP4 (Fig. 8B).

DISCUSSION

We have shown that *Tshz3* is expressed as early as E11.5 in the mesenchyme around the UB stalk, but that its function appears to be dispensable for ureter development until E14.5, when SMCs differentiation starts. Indeed, in the absence of TSHZ3, early events, such as proliferation and condensation of the undifferentiated mesenchymal cells around the distal UB, occur properly. However, the differentiation program triggered by the activation of SM factors, such as SMAA or SM22A, is impeded. Furthermore, our ex vivo data support the contention that hydronephrosis results from functional urinary flow impairment caused by defective ureteric contractility. Studies of (non-ureteric) mesenchymal cells suggest that SM differentiation depends on the ability of serum response factor to recruit its transcriptional co-activator myocardin (Pipes et al., 2006). We show that myocardin is expressed in wild-type ureteric SMC, validating the previously reported *Myocd* upregulation during mouse ureteric maturation (Mitchell et al., 2006). Our findings that, in the *Tshz3* mutant, expression of myocardin is lost in SM precursor cells enables us to propose that TSHZ3 plays an important role in the induction of transcriptional programs that regulate SMCs differentiation.

Tshz3 and radial patterning

During ureter morphogenesis, Tshz3 was detected in the undifferentiated mesenchymal cells that contribute to the SM, the adventitia and the stromal layers. So far, very few genes have been implicated in the reciprocal signals that trigger the specification, proliferation and differentiation of epithelial and mesenchymal compartments. However, *Shh*, *Bmp4* and *Tbx18* appear to have crucial roles in the development of both compartments. SHH signalling is also required for establishing and/or maintaining the stromal cells, a mesenchymal cell population of undefined origin (Mahoney et al., 2006; Yu et al., 2002). In *Tshz3* mutant ureters, expression of RALDH2 indicates

that differentiation of stromal cells occurs properly, suggesting that the sub-epithelial mesenchymal cells are SHH-responsive. Analysis of the *Tshz3*$^{lacZ/lacZ}$ mutant ureters indicates that differentiation of the epithelium also occurs normally, and suggests that this cannot depend on the differentiation of the SMCs themselves, but rather on earlier events, as has been suggested by *Bmp4* loss of function analyses (Brenner-Anantharam et al., 2007). Our data also show that TSHZ3 is dispensable for recruitment and condensation steps (see Fig. S2G,H in the supplementary material) before SM differentiation itself (Raatikainen-Ahokas et al., 2000). Therefore, the *Tshz3* mutant provides a unique genetic tool in which stromal and urothelial differentiation, and also mesenchymal recruitment and condensation, are uncoupled from differentiation of SMCs.

In vivo, urothelial *Shh* was expressed as normal in mutants, which had overtly responsive adjacent mesenchymal cells, as shown by *Ptch1* expression and indices of proliferation in the latter compartment. Furthermore, BMP4 signalling was initiated as normal in *Tshz3* mutant ureters, as assessed by expression of *Bmp4* and pSMAD1/5/8 in cells around ureteric urothelia. Nevertheless, *Tshz3*-null mutation specifically impaired the differentiation of SMC progenitors in proximal uterers in vivo, and, ex vivo, exogenous BMP4 treatment did not rescue *Tshz3* mutant proximal ureter SMC differentiation, as assessed by SMAA expression. Before E12.5, when BMP4 signalling is essential for SMC differentiation (Brenner-Anantharam et al., 2007), TSHZ3 was expressed by SM progenitors and we showed that, in renal tract explants, *Tshz3* expression was enhanced upon BMP4 treatment. These results support the idea that *Tshz3* is downstream of BMP4 and might even be a direct target of BMP4 signalling.

Several studies suggest that BMP4 is not the only signal necessary for ureteric SM differentiation and it is possible that TSHZ3 is required for these other signals (Airik and Kispert, 2007; Chang et al., 2004; Miyazaki et al., 2003; Yu et al., 2002). The molecular mechanisms whereby developmental signals modulate the regulatory network for SM gene transcription warrants further studies. In vivo, loss of *Tshz3* leads to the absence of myocardin and in vitro BMP4 stimulate *Tshz3* and *Myocd* expression. This study suggests that Tshz3 could serve as a central transcriptional factor that integrates BMP4 signalling into the transcriptional regulatory network by controlling the expression of myocardin, a key factor for SM differentiation.

Regionalisation of the ureter

Tshz3 is evenly expressed in the mesenchyme along the entire proximodistal axis of the ureter. However, in the absence of *Tshz3*, SM markers were strongly downregulated in the proximal ureter and SM failed to develop, whereas in the distal part of the ureter, weak expression of SM proteins appears sufficient to produce functional SM. Therefore, our data show that the proximal and distal parts of the ureter respond differently to the absence of *Tshz3*, and hence show that the ureter is regionalised along its length. Temporal regionalisation of the ureter along the proximodistal axis is supported by the observation that SM differentiation occurs in a wave from the kidney to the bladder (Yu et al., 2002). However, no mesenchymal transcription factors differentially expressed along the ureter have been found, which could support a spatial regionalisation of this structure. According to its broad expression, it is unlikely that TSHZ3 alone differentially controls gene expression in a proximodistal gradient but it might well act as a co-factor of an essential regionalised factor or be recruited by a signalling pathway that acts locally. Therefore, our *Tshz3*-null mutant constitutes an excellent tool for the identification of such regionalised factors.

Tshz3 mutant is a model for functional obstruction linked to SM impairment

The lack of *Tshz3* is associated with bilateral hydronephrosis and proximal hydroureter, with an onset before birth. This mouse phenotype is reminiscent of human congenital PUJO, a common birth defect that is sometimes associated with significant kidney damage caused by urinary flow impairment (Decramer et al., 2006; Gunn et al., 1995; Ismaili et al., 2006). PUJO ureters are not anatomically blocked, but have aberrantly arranged SM in the region where the proximal ureter joins the renal pelvis (dell'Agnola et al., 1990; Zhang et al., 2000). In an intriguing parallel, we found that in *Tshz3*$^{lacZ/lacZ}$ mice, SMC differentiation was impaired in the proximal ureter. Thus, we postulate that the gross phenotypes of both *Tshz3*$^{lacZ/lacZ}$ mice and human PUJO result from a failure of peristalsis in the region of the proximal ureter, which leads to 'functional' urine flow impairment. Recently, other mouse models for congenital hydronephrosis with defects in SM have been generated. Mutants for *Shh* and *Tbx18* affect both urothelium and SMC. Loss of *Dlgh1* perturbs the orientation of the SMCs, causes a slight delay in SMC maturation, and causes stromal cell defects (Mahoney et al., 2006). Finally, inactivation of *Cnb1*, as well as *At1*, causes obstruction after birth by affecting postnatal proliferation and maturation of pelvic SMCs (Chang et al., 2004; Miyazaki et al., 1998). The *Tshz3* mutant will be useful for analysing prenatal functional kidney obstruction that results from incomplete SMC differentiation in the absence developmental defects of other ureteric cell populations. Mouse models have guided candidate gene screens for identification of mutations causing human urinary tract malformations (Jenkins and Woolf, 2007; Lu et al., 2007). We suggest that *TSHZ3* should be examined as a candidate for congenital PUJO and related disorders, such as multicystic dysplastic kidney, a disorder characterised by severely disorganised ureteric and renal pelvic morphogenesis (Woolf et al., 2004).

The work was supported by the Biotechnology and Biological Sciences Research Council, the British Council, The Company of Biologists, Egide Alliance Program, the Association Française contre les Myopathies and Kids Kidney Research. We thank J. P. Chauvin for assistance with transmission electronic microscopy experiments, D. Rampling for performing Masson's trichrome staining and K. Mesbah for advice on immunohistochemistry. We thank J. Davies, A. Dimovski, Z. Gucev, T. Lecuit and V. Tasic for helpful discussions.

Supplementary material

Supplementary material for this article is available at
http://dev.biologists.org/cgi/content/full/135/19/3301/DC1

References

Airik, R. and Kispert, A. (2007). Down the tube of obstructive nephropathies: the importance of tissue interactions during ureter development. *Kidney Int.* **72**, 1459-1467.

Airik, R., Bussen, M., Singh, M. K., Petry, M. and Kispert, A. (2006). Tbx18 regulates the development of the ureteral mesenchyme. *J. Clin. Invest.* **116**, 663-674.

Breiteneder-Geleff, S., Matsui, K., Soleiman, A., Meraner, P., Poczewski, H., Kalt, R., Schaffner, G. and Kerjaschki, D. (1997). Podoplanin, novel 43-kd membrane protein of glomerular epithelial cells, is down-regulated in puromycin nephrosis. *Am. J. Pathol.* **151**, 1141-1152.

Brenner-Anantharam, A., Cebrian, C., Guillaume, R., Hurtado, R., Sun, T. T. and Herzlinger, D. (2007). Tailbud-derived mesenchyme promotes urinary tract segmentation via BMP4 signaling. *Development* **134**, 1967-1975.

Burgu, B., McCarthy, L. S., Shah, V., Long, D. A., Wilcox, D. T. and Woolf, A. S. (2006). Vascular endothelial growth factor stimulates embryonic urinary bladder development in organ culture. *BJU Int.* **98**, 217-225.

Caubit, X., Tiveron, M. C., Cremer, H. and Fasano, L. (2005). Expression patterns of the three Teashirt-related genes define specific boundaries in the developing and postnatal mouse forebrain. *J. Comp. Neurol.* **486**, 76-88.

Chang, C. P., McDill, B. W., Neilson, J. R., Joist, H. E., Epstein, J. A., Crabtree, G. R. and Chen, F. (2004). Calcineurin is required in urinary tract mesenchyme

for the development of the pyeloureteral peristaltic machinery. *J. Clin. Invest.* **113**, 1051-1058.
Chung, K. H. and Chevalier, R. L. (1996). Arrested development of the neonatal kidney following chronic ureteral obstruction. *J. Urol.* **155**, 1139-1144.
Decramer, S., Wittke, S., Mischak, H., Zurbig, P., Walden, M., Bouissou, F., Bascands, J. L. and Schanstra, J. P. (2006). Predicting the clinical outcome of congenital unilateral ureteropelvic junction obstruction in newborn by urinary proteome analysis. *Nat. Med.* **12**, 398-400.
dell'Agnola, C. A., Carmassi, L. M., Merlo, D. and Tadini, B. (1990). Duration and severity of congenital hydronephrosis as a cause of smooth muscle deterioration in pyelo-ureteral junction obstruction. *Z. Kinderchir.* **45**, 286-290.
Denholm, B., Sudarsan, V., Pasalodos-Sanchez, S., Artero, R., Lawrence, P., Maddrell, S., Baylies, M. and Skaer, H. (2003). Dual origin of the renal tubules in Drosophila: mesodermal cells integrate and polarize to establish secretory function. *Curr. Biol.* **13**, 1052-1057.
Ek, S., Lidefeldt, K. J. and Varricio, L. (2007). Fetal hydronephrosis; prevalence, natural history and postnatal consequences in an unselected population. *Acta Obstet. Gynecol. Scand.* **86**, 1463-1466.
Gunn, T. R., Mora, J. D. and Pease, P. (1995). Antenatal diagnosis of urinary tract abnormalities by ultrasonography after 28 weeks' gestation: incidence and outcome. *Am. J. Obstet. Gynecol.* **172**, 479-486.
Hoyer, J. R., Resnick, J. S., Michael, A. F. and Vernier, R. L. (1974). Ontogeny of Tamm-Horsfall urinary glycoprotein. *Lab. Invest.* **30**, 757-761.
Huang, J., Cheng, L., Li, J., Chen, M., Zhou, D., Lu, M. M., Proweller, A., Epstein, J. A. and Parmacek, M. S. (2008). Myocardin regulates expression of contractile genes in smooth muscle cells and is required for closure of the ductus arteriosus in mice. *J. Clin. Invest.* **118**, 515-525.
Ismaili, K., Hall, M., Piepsz, A., Wissing, K. M., Collier, F., Schulman, C. and Avni, F. E. (2006). Primary vesicoureteral reflux detected in neonates with a history of fetal renal pelvis dilatation: a prospective clinical and imaging study. *J. Pediatr.* **148**, 222-227.
Jen, Y., Manova, K. and Benezra, R. (1996). Expression patterns of Id1, Id2, and Id3 are highly related but distinct from that of Id4 during mouse embryogenesis. *Dev. Dyn.* **207**, 235-252.
Jenkins, D. and Woolf, A. S. (2007). Uroplakins: new molecular players in the biology of urinary tract malformations. *Kidney Int.* **71**, 195-200.
Kelley, C. A., Kawamoto, S., Conti, M. A. and Adelstein, R. S. (1991). Phosphorylation of vertebrate smooth muscle and nonmuscle myosin heavy chains in vitro and in intact cells. *J. Cell. Sci.* **Suppl. 14**, 49-54.
Laugier, E., Yang, Z., Fasano, L., Kerridge, S. and Vola, C. (2005). A critical role of teashirt for patterning the ventral epidermis is masked by ectopic expression of tiptop, a paralog of teashirt in Drosophila. *Dev. Biol.* **283**, 446-458.
Li, J., Shiroyanagi, Y., Lin, G., Haqq, C., Lin, C. S., Lue, T. F., Willingham, E. and Baskin, L. S. (2006). Serum response factor, its cofactors, and epithelial-mesenchymal signaling in urinary bladder smooth muscle formation. *Differentiation* **74**, 30-39.
Li, S., Wang, D. Z., Wang, Z., Richardson, J. A. and Olson, E. N. (2003). The serum response factor coactivator myocardin is required for vascular smooth muscle development. *Proc. Natl. Acad. Sci. USA* **100**, 9366-9370.
Lu, W., van Eerde, A. M., Fan, X., Quintero-Rivera, F., Kulkarni, S., Ferguson, H., Kim, H. G., Fan, Y., Xi, Q., Li, Q. G. et al. (2007). Disruption of ROBO2 is associated with urinary tract anomalies and confers risk of vesicoureteral reflux. *Am. J. Hum. Genet.* **80**, 616-632.
Mahoney, Z. X., Sammut, B., Xavier, R. J., Cunningham, J., Go, G., Brim, K. L., Stappenbeck, T. S., Miner, J. H. and Swat, W. (2006). Discs-large homolog 1 regulates smooth muscle orientation in the mouse ureter. *Proc. Natl. Acad. Sci. USA* **103**, 19872-19877.
Manfroid, I., Caubit, X., Kerridge, S. and Fasano, L. (2004). Three putative murine Teashirt orthologues specify trunk structures in Drosophila in the same way as the Drosophila teashirt gene. *Development* **131**, 1065-1073.
Mansour, S. L., Thomas, K. R. and Capecchi, M. R. (1988). Disruption of the proto-oncogene int-2 in mouse embryo-derived stem cells: a general strategy for targeting mutations to non-selectable genes. *Nature* **336**, 348-352.
Marples, D., Knepper, M. A., Christensen, E. I. and Nielsen, S. (1995). Redistribution of aquaporin-2 water channels induced by vasopressin in rat kidney inner medullary collecting duct. *Am. J. Physiol.* **269**, C655-C664.
Massague, J., Seoane, J. and Wotton, D. (2005). Smad transcription factors. *Genes Dev.* **19**, 2783-2810.
McHugh, K. M. (1995). Molecular analysis of smooth muscle development in the mouse. *Dev. Dyn.* **204**, 278-290.
Mendelsohn, C. (2004). Functional obstruction: the renal pelvis rules. *J. Clin. Invest.* **113**, 957-959.
Mendelsohn, C. (2006). Going in circles: conserved mechanisms control radial patterning in the urinary and digestive tracts. *J. Clin. Invest.* **116**, 635-637.
Mitchell, E. K., Taylor, D. F., Woods, K., Davis, M. J., Nelson, A. L., Teasdale, R. D., Grimmond, S. M., Little, M. H., Bertram, J. F. and Caruana, G. (2006). Differential gene expression in the developing mouse ureter. *Gene Expr. Patterns* **6**, 519-538.
Miyazaki, Y., Tsuchida, S., Nishimura, H., Pope, J. C. t., Harris, R. C., McKanna, J. M., Inagami, T., Hogan, B. L., Fogo, A. and Ichikawa, I. (1998). Angiotensin induces the urinary peristaltic machinery during the perinatal period. *J. Clin. Invest.* **102**, 1489-1497.
Miyazaki, Y., Oshima, K., Fogo, A., Hogan, B. L. and Ichikawa, I. (2000). Bone morphogenetic protein 4 regulates the budding site and elongation of the mouse ureter. *J. Clin. Invest.* **105**, 863-873.
Miyazaki, Y., Oshima, K., Fogo, A. and Ichikawa, I. (2003). Evidence that bone morphogenetic protein 4 has multiple biological functions during kidney and urinary tract development. *Kidney Int.* **63**, 835-844.
Mombaerts, P., Wang, F., Dulac, C., Chao, S. K., Nemes, A., Mendelsohn, M., Edmondson, J. and Axel, R. (1996). Visualizing an olfactory sensory map. *Cell* **87**, 675-686.
Owens, G. K. (1995). Regulation of differentiation of vascular smooth muscle cells. *Physiol. Rev.* **75**, 487-517.
Pipes, G. C., Creemers, E. E. and Olson, E. N. (2006). The myocardin family of transcriptional coactivators: versatile regulators of cell growth, migration, and myogenesis. *Genes Dev.* **20**, 1545-1556.
Raatikainen-Ahokas, A., Hytonen, M., Tenhunen, A., Sainio, K. and Sariola, H. (2000). BMP-4 affects the differentiation of metanephric mesenchyme and reveals an early anterior-posterior axis of the embryonic kidney. *Dev. Dyn.* **217**, 146-158.
Relaix, F., Rocancourt, D., Mansouri, A. and Buckingham, M. (2004). Divergent functions of murine Pax3 and Pax7 in limb muscle development. *Genes Dev.* **18**, 1088-1105.
Schedl, A. (2007). Renal abnormalities and their developmental origin. *Nat. Rev. Genet.* **8**, 791-802.
Schmidt-Ott, K. M., Chen, X., Paragas, N., Levinson, R. S., Mendelsohn, C. L. and Barasch, J. (2006). c-kit delineates a distinct domain of progenitors in the developing kidney. *Dev. Biol.* **299**, 238-249.
Sharma, M., Fopma, A., Brantley, J. G. and Vanden Heuvel, G. B. (2004). Coexpression of Cux-1 and Notch signaling pathway components during kidney development. *Dev. Dyn.* **231**, 828-838.
Shepherd, T. G., Theriault, B. L. and Nachtigal, M. W. (2008). Autocrine BMP4 signalling regulates ID3 proto-oncogene expression in human ovarian cancer cells. *Gene* **414**, 95-105.
Tena, J. J., Neto, A., de la Calle-Mustienes, E., Bras-Pereira, C., Casares, F. and Gomez-Skarmeta, J. L. (2007). Odd-skipped genes encode repressors that control kidney development. *Dev. Biol.* **301**, 518-531.
Vanden Heuvel, G. B., Bodmer, R., McConnell, K. R., Nagami, G. T. and Igarashi, P. (1996). Expression of a cut-related homeobox gene in developing and polycystic mouse kidney. *Kidney Int.* **50**, 453-461.
Wang, D. Z. and Olson, E. N. (2004). Control of smooth muscle development by the myocardin family of transcriptional coactivators. *Curr. Opin. Genet. Dev.* **14**, 558-566.
Winyard, P. J., Risdon, R. A., Sams, V. R., Dressler, G. R. and Woolf, A. S. (1996). The PAX2 tanscription factor is expressed in cystic and hyperproliferative dysplastic epithelia in human kidney malformations. *J. Clin. Invest.* **98**, 451-459.
Woolf, A. S., Price, K. L., Scambler, P. J. and Winyard, P. J. (2004). Evolving concepts in human renal dysplasia. *J. Am. Soc. Nephrol.* **15**, 998-1007.
Yu, J., Carroll, T. J. and McMahon, A. P. (2002). Sonic hedgehog regulates proliferation and differentiation of mesenchymal cells in the mouse metanephric kidney. *Development* **129**, 5301-5312.
Zhang, F., Nakanishi, G., Kurebayashi, S., Yoshino, K., Perantoni, A., Kim, Y. S. and Jetten, A. M. (2002). Characterization of Glis2, a novel gene encoding a Gli-related, Kruppel-like transcription factor with transactivation and repressor functions. Roles in kidney development and neurogenesis. *J. Biol. Chem.* **277**, 10139-10149.
Zhang, P. L., Peters, C. A. and Rosen, S. (2000). Ureteropelvic junction obstruction: morphological and clinical studies. *Pediatr. Nephrol.* **14**, 820-826.

Table S1. Proliferation and apoptosis in embryonic proximal ureters

Proliferation	E15 (+/+)	E15 (–/–)	E16 (+/+)	E16 (–/–)
Urothelia	13.2±4.3	9.92±6.0	11.7±4.8	6.3±0.62
Aggregated mesenchyme	7.9±3.8	4.3±1.9	2.1±1.5	2.3±0.64
Loose mesenchyme	9.5±1.3	11.3±2.9	6.4±3.3	4.9±1.3
Apoptosis	**E15 (+/+)**	**E15 (–/–)**	**E16 (+/+)**	**E16 (–/–)**
Urothelia	0.47±0.33	0.09±0.09	0.42±0.42	0.09±0.09
Aggregated mesenchyme	0.00±0.00	0.00±0.00	0.00±0.00	0.00±0.00
Loose mesenchyme	0.12±0.07	0.16±0.16	0.00±0.00	0.05±0.05

Point prevalence of proliferation (% PCNA-positive cells) and apoptosis (% TUNEL-positive cells) showed that the percentage point prevalence of positive nuclei in urothelia, condensed mesenchyme (containing presumptive SMCs) near the urothelium and looser mesenchyme outside this zone, was not significantly different in wild-type versus null mutant proximal ureters at both E15.5 (before the onset of hydroneprosis) and also at E16.5 (when hydronephrosis was present). Data are expressed as mean±s.e.m. with n=3 or 4 for each experimental group.